

His166 Is the Schiff Base Proton Acceptor in Attractant Phototaxis Receptor Sensory Rhodopsin I

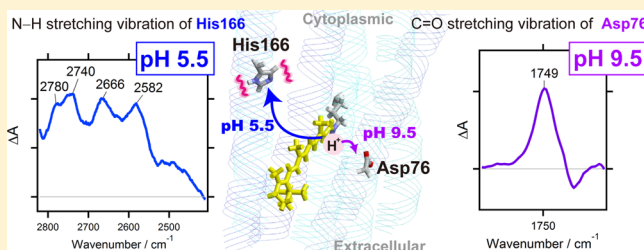
Jun Sasaki,[†] Hazuki Takahashi,[†] Yuji Furutani,^{†,||} Oleg A. Sineshchekov,[‡] John L. Spudich,[‡] and Hideki Kandori^{*,†,§}

[†]Department of Frontier Materials, Nagoya Institute of Technology, Showa-ku, Nagoya 466-8555, Japan

[‡]Center for Membrane Biology, Department of Biochemistry and Molecular Biology, University of Texas Health Science Center, Houston, Texas 77030, United States

[§]OptoBioTechnology Research Center, Nagoya Institute of Technology, Showa-ku, Nagoya 466-8555, Japan

ABSTRACT: Photoactivation of attractant phototaxis receptor sensory rhodopsin I (SRI) in *Halobacterium salinarum* entails transfer of a proton from the retinylidene chromophore's Schiff base (SB) to an unidentified acceptor residue on the cytoplasmic half-channel, in sharp contrast to other microbial rhodopsins, including the closely related repellent phototaxis receptor SRII and the outward proton pump bacteriorhodopsin, in which the SB proton acceptor is an aspartate residue salt-bridged to the SB in the extracellular (EC) half-channel. His166 on the cytoplasmic side of the SB in SRI has been implicated in the SB proton transfer reaction by mutation studies, and mutants of His166 result in an inverted SB proton release to the EC as well as inversion of the protein's normally attractant phototaxis signal to repellent. Here we found by difference Fourier transform infrared spectroscopy the appearance of Fermi-resonant X–H stretch modes in light-minus-dark difference spectra; their assignment with ¹⁵N labeling and site-directed mutagenesis demonstrates that His166 is the SB proton acceptor during the photochemical reaction cycle of the wild-type SRI–HtrI complex.



Microbial rhodopsins are widespread photoactive proteins that function as light-driven ion transporters and light sensors for phototaxis and other photosensory behavior in prokaryotic and eukaryotic microorganisms.^{1–4} They contain seven transmembrane helices that form a pocket for the chromophore retinal, which is covalently attached in a protonated Schiff base (PSB) linkage to a lysyl residue on the seventh helix. Retinal photoisomerization from all-*trans* to 13-*cis* initiates a photochemical reaction cycle that typically includes, in both rhodopsin proton pumps and transducer-free sensory rhodopsin I, transfer of the Schiff base proton to a conserved carboxylate acceptor, Asp or Glu, on the third helix.

In the light-driven proton pump bacteriorhodopsin (BR),^{4–6} the pivotal components of the mechanism are two Asp residues in the proton conduction channel, one salt-bridged to the PSB on the extracellular (EC) side and another located in the cytoplasmic (CP) side of the half-channel with respect to the PSB. Outward proton current is produced through proton relays in the channel upon breakage of the salt bridge as a result of photoisomerization of the retinal chromophore, first from the PSB to the Asp on the EC side (the acceptor Asp85) and the second from the Asp on the CP side (the donor Asp96) to the SB. The spectral photocycle intermediate with deprotonated SB exhibits a far blue-shifted absorption band in the near-UV designated the M (for “metarhodopsin”) intermediate. Following intrachannel proton relays, the release of a proton to the external milieu from the extracellular side and uptake by the

unprotonated donor Asp from the cytoplasm complete the net translocation of a proton across the membrane.

Sensory rhodopsins (SRs), the best studied of which are the phototaxis receptors in haloarchaea (sensory rhodopsins I and II), conserve the carboxylic acid residue (Asp) corresponding to the acceptor Asp85 in BR, but not that of the proton donor Asp96. Haloarchaeal SRI and SRII mediate orange-light attractant and blue-light repellent phototaxis in complex with their respective transducer molecules HtrI and HtrII. Opposite consequences of the signaling by SRI and SRII in response to photostimuli have been attributed to opposite conformational changes of the receptors based primarily on the direction of their SB proton movements^{7,8} and confirmed by electron paramagnetic resonance spectroscopy.⁹ The repellent signaling SRII–HtrII complex exhibits EC side-directed deprotonation,^{7,8,10} as in proton pumps, and the residue corresponding to Asp85 in BR serves as the PSB proton acceptor.¹¹ Repellent signaling mutants of the SRI–HtrI complex (inverted mutants) also deprotonate to the conserved EC Asp,^{7,8,12–14} however, the wild-type attractant signaling SRI–HtrI complex exhibits CP-directed PSB deprotonation.^{7–9}

His166 was shown to play a crucial role in proton transfer, phototaxis signaling, and the direction of SB deprotonation in the

Received: July 7, 2014

Revised: August 27, 2014

Published: August 27, 2014

SRI–HtrI complex^{7,15} and hence was suggested as the most likely candidate for the cytoplasmic SB proton acceptor. Here we confirm this suggestion with Fourier transform infrared (FTIR) spectroscopy and also investigate the influence of mutation of the proton acceptor on the PSB deprotonation in the SRI–HtrI complex.

MATERIALS AND METHODS

The gene of the SRI–HtrI fusion protein, in which the C-terminus of SRI is joined through a flexible linker peptide (ASASNGASA) to the N-terminus of HtrI truncated at position 147 fused to a hexahistidine tag at the C-terminus (SRI–HtrI₁₄₇), was cloned into expression vector pET-21d (Novagen) under the control of the T7 promoter as described previously.¹⁶ The expression of the gene in BL21(DE3) was induced by addition of 1 mM isopropyl β -D-thiogalactopyranoside and 5 μ M all-*trans*-retinal. The [¹⁵N₃]His-labeled SRI–HtrI₁₄₇ fusion protein was grown in M9 medium containing [¹⁵N₃]His (100 mg/L) according to the method described previously,¹⁷ and mutant proteins were prepared as described previously.¹² Briefly, membranes containing the SRI–HtrI₁₄₇ complex were solubilized with 2.0% *n*-dodecyl β -D-maltoside (DDM) and purified by Ni-NTA chromatography. The SRI–HtrI₁₄₇ fusion protein was then reconstituted into 1- α -phosphatidylglycerol (PG) liposomes (1:50 SRI:PG molar ratio), through removal of DDM with Bio-Beads (SM-2, Bio-Rad). The proteoliposomes were washed three times with 2 mM citrate buffer (pH 5.5) or 2 mM borate (pH 9.5) containing 300 mM NaCl. The sediment obtained after the third centrifugation was deposited on a BaF₂ window 18 mm in diameter and was dried slowly at room temperature under high humidity.¹²

Low-temperature FTIR spectroscopy was performed as described previously.^{18,19} After hydration of the dried film of the proteoliposome with 1–2 μ L of H₂O, the sample was sealed with another BaF₂ window with a 1 mm thick spacer between them, which was then mounted in an Oxford Optistat-DN cryostat placed into an FTS-7000 spectrometer (DIGILAB). Illumination from a 1 kW halogen–tungsten lamp was passed through a cutoff filter (VY-50, Toshiba) to produce >480 nm light, which was directed to the sample to convert SRI into M at 260 K. The spectra were constructed from 128 interferograms with a spectral resolution of 2 cm^{–1}. The M-minus-SRI difference spectrum was calculated by subtracting the spectrum recorded before the illumination from the spectra recorded after the illumination. Three difference spectra were averaged to yield the final difference spectrum. All spectra were normalized with the C–C stretching vibration of the retinal chromophore at 1197 cm^{–1}.

Attenuated total reflection (ATR) FTIR spectroscopy was performed with an FTS-6000 spectrometer (DIGILAB) equipped with a diamond ATR crystal sample cell (SMITHS, nine effective internal reflections).¹³ 4-Methylimidazole was dissolved in an aqueous solution, with the pH value adjusted by adding HCl or NaOH.

Photoinduced electrical measurements were performed as described previously.^{7,10} Briefly, BL21(DE3) cells expressing the SRI–HtrI₁₄₇ fusion protein with or without mutations suspended in the measuring buffer containing 5 mM Tris-HCl (pH 7.0), 1.5 mM NaCl, 0.15 mM CaCl₂, and 0.15 mM MgSO₄ were placed in a rectangular plastic cuvette with two platinum electrodes. The sample was flashed with a Nd:YAG Surelite-I laser (532 nm, 6 ns pulse; Continuum) along the line between two platinum electrodes. A macroscopic electrical current in the cuvette

appeared because of the asymmetric absorption of light in each bacterial cell. The electrode remote from the light source was fed into a low-noise current amplifier (model 428, Keithley) with a rise time of 2 μ s. The signals were digitized and stored by using the DIGIDATA 1325A and pCLAMP 9.0 program (both from Axon Instruments). Twenty to 150 signals with a maximal sampling rate of 2 μ s/point were averaged.

RESULTS

PSB Deprotonation When the EC Side Acceptor Asp76 Is Protonated or Unprotonated. At pH values higher than the pK_a of Asp76 (~8.5), the PSB in the SRI–HtrI complex has been shown to transfer its proton to Asp76 upon light conversion to the M state when Asp76 is unprotonated in the unphotolyzed state (e.g., in the HtrI-free or alkaline form of SRI).²⁰ This proton transfer is evident in FTIR spectra from the appearance of the C=O stretching vibrational mode of a protonated carboxylic acid at 1749 cm^{–1} that was assigned earlier to that of Asp76 in the difference FTIR spectrum between M and SRI at pH 9.5¹² and correlates with increased outwardly directed photocurrent at high pH.⁷ The FTIR spectrum is reproduced in Figure 1a (dotted

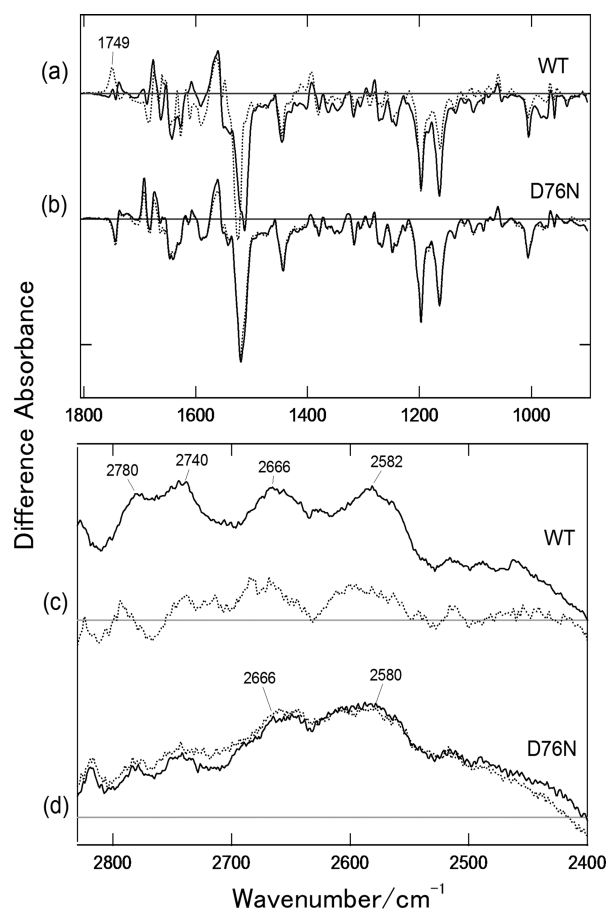


Figure 1. M-minus-SRI difference FTIR spectra of the SRI–HtrI complex measured at pH 5.5 (—) and pH 9.5 (···) for the wild-type (a and c) and D76N mutant SRIs (b and d). The SRI–HtrI complex in the acidic and alkaline forms in the hydrated film sample in a PG lipid membrane was illuminated with >480 nm light to produce the M state. Spectra were normalized to the C–C stretching vibration amplitude of the retinal chromophore at 1197 cm^{–1}. The vertical scale of the y-axis is 0.015 au in the top panel (a and b) and 0.00114 au in the bottom panel (c and d).

line) along with the corresponding difference spectrum measured at pH 5.5 (solid line). At physiological or lower pH values, Asp76 is protonated in the unphotolyzed state and cannot accept the proton from the PSB, which is reflected in the difference FTIR spectrum devoid of the positive band at 1749 cm^{-1} (Figure 1a, solid line). The minor bilobed bands in the frequency domain between 1800 and 1700 cm^{-1} appearing in the difference spectrum of the acidic form have been attributed to perturbations of one or more protonated carboxylic residues, including Asp76, because of the environmental changes.^{12,21} The lack of a positive band essentially excludes a carboxylic acid residue as the proton acceptor from the PSB in the acidic form.

In D76N of SRI (SRI/D76N–HtrI), which mediates attractant phototaxis signaling like the wild type,²² the pH-dependent alterations of the SB proton acceptor are abolished, as evidenced by the M-minus-SRI difference FTIR spectra of the HtrI–SRI/D76N complex (Figure 1b) showing overall analogy in the spectral features at both pH 5.5 and 9.0 to that of the acidic form of the wild-type SRI–HtrI complex (Figure 1a). Newly appearing bands near 1750 – 1720 cm^{-1} can be ascribed to the perturbation of Asn76 due to the environmental changes upon photoconversion from SRI to M.^{12,21}

Vibrational Bands That Can be Attributed to the SB Proton Acceptor in the Acidic Form of SRI. Vibrational modes that can be attributed to the proton acceptor of the SB in the acidic form of SRI should appear on the positive side of the M-minus-SRI spectrum of wild-type SRI only in the acidic form but not in the alkaline form. In HtrI-complexed SRI/D76N, the appearance of the corresponding bands is expected at both pH 5.5 and 9.5. Bands fulfilling such requirements appear on the positive side of the M-minus-SRI difference FTIR spectrum as a broad feature with subpeaks in the frequency domain between 2800 and 2400 cm^{-1} only in the acidic form of HtrI-complexed SRI but not in the alkaline form (Figure 1c). Stretching vibrational modes of N–H, O–H, or C–H groups forming enormously strong hydrogen bonds contribute to the bands in the frequency domain. Such broad features are also seen in the M-minus-SRI difference FTIR spectra of HtrI-free SRI in the acidic form but not in the alkaline form (data not shown) and also in HtrI-complexed SRI/D76N at both pH 5.5 and 9.5 (Figure 1d), with some differences in the intensity and the frequency of sub-bands compared to those of the bands of the wild type.

Assignment of the Broad-Featured Band between 2800 and 2400 cm^{-1} . A histidine residue is a candidate for the proton acceptor of the SB because its imidazole side chain is possibly in a singly protonated neutral form capable of being protonated near neutral pH values and also because protonated histidine residues with strong hydrogen bonding have been shown to exhibit analogous broad-featured bands in the primary quinone acceptor Q_A of photosystem II (PSII) upon photo-reduction.^{23,24} His166 has been suggested as a possible SB proton acceptor in the SRI–HtrI complex primarily on the basis of the finding that its mutation to any of seven different residues greatly reduces the flash yield of M and inverts the direction of SB proton transfer upon formation of the M intermediate.^{7,15} We produced the [^{15}N]histidine-labeled SRI–HtrI complex to aid in the identification of the broad-featured bands. Confirming that protonation of a histidine residue occurs, each of the sub-bands in the M-minus-SRI difference FTIR spectrum of the acidic form of the SRI–HtrI complex exhibited downshifts of ~ 15 – 20 cm^{-1} in the labeled sample (Figure 2, top panel), and the extents of the isotope shifts are almost identical with those observed

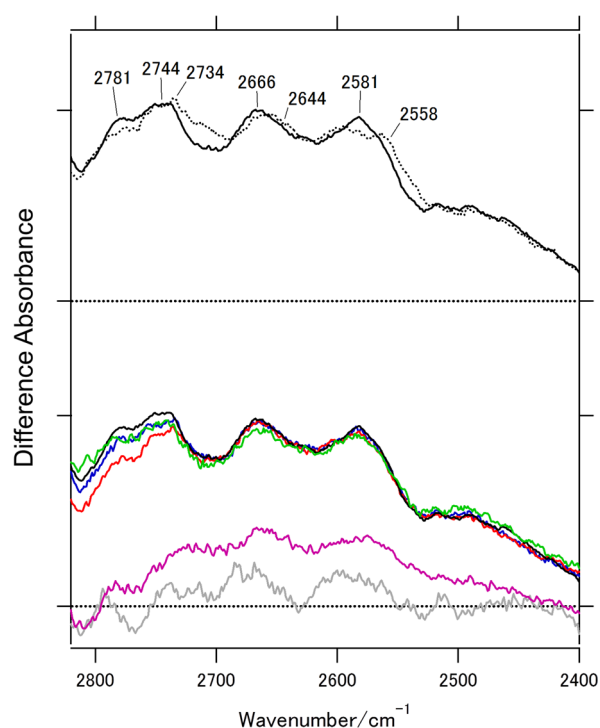


Figure 2. M-minus-SRI difference FTIR spectra of the SRI–HtrI complex in the acidic form (pH 5.5): (top) unlabeled (—) and [^{15}N]His-labeled (···) protein and (bottom) wild type (black), H34A (blue), H135A (red), H166L (purple), and H221A (green) mutant proteins of the SRI in complex with HtrI. The spectrum of the wild type at pH 9.5 is also shown (gray). One division of the y-axis is 0.0004 au.

previously,^{23,24} identifying the peaks as originating from N–H stretching vibrational modes of a histidine side chain. Our interpretation is that at least one of the two imidazole nitrogens becomes protonated upon formation of M (i.e., not in the imidazolate form).

To compare spectral features of the N–H stretching mode of the imidazole side chain in its neutral form (singly protonated form) and in its cationic form (imidazolium), a model compound, 4-methylimidazole (MeIm), in aqueous solution at pH 5.1, 8.6, and 10.1 adjusted by adding HCl, was subjected to ATR-FTIR (Figure 3). Only at pH 5.1, well below the pK_a of the protonation to the second nitrogen in the imidazole ring (pH ~ 7), do broad features at $>2500\text{ cm}^{-1}$ (Figure 3, inset) similar to those observed on the positive side of M-minus-SRI spectra become obvious on top of the large background absorption caused by water, whereas the spectra measured at pH 8.6 and 10.1, the pH values between the two pK_a values for the double protonation (pH ~ 7) and for the single protonation (pH ~ 14.5), show negligibly small bands (Figure 3 and the inset), indicating that the broad-featured bands can be attributed to a strongly hydrogen-bonded N–H stretching mode of the cationic form of imidazole. Hence, the appearance of the analogous positive feature in the M-minus-SRI spectrum in the acidic form can be attributed to protonation of the second nitrogen (imidazolium formation) in one or more histidine side chains of SRI upon formation of M.

Assignment to a Specific Histidine Residue. To address which of the four histidine residues (His34, His135, His166, and His221) in SRI accepts the proton from the PSB, we conducted FTIR measurements on SRI mutants in which each of the four histidine residues was mutated to Ala except for His166, which

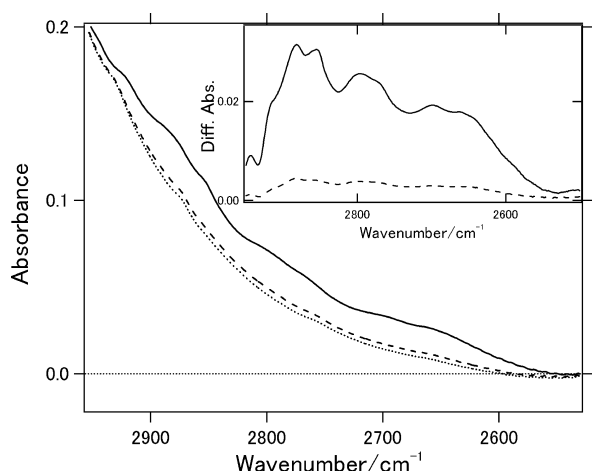


Figure 3. ATR-FTIR spectra of 4-methylimidazole in aqueous solution at pH 5.1 (—), 8.6 (---), and 10.1 (···) in the region of 2900–2500 cm^{-1} . The differences with respect to the spectrum at pH 10.1 for the spectra at pH 5.1 (—) and 8.6 (---) are shown in the inset.

was replaced with Leu because H166A did not survive purification.

In the bottom panel of Figure 2, M-minus-SRI FTIR spectra in the frequency domain of 2800–2400 cm^{-1} are compared between wild-type SRI and the four mutants (H34A, H135A, H166L, and H221A). As is evident from the almost super-imposable spectra of H34A, H135A, and H221A, the positive N–H stretching modes do not contribute to the groups of the bands in the frequency domain, ruling out the possibility that any one of these three residue is the proton acceptor of the PSB. On the other hand, the M-minus-SRI FTIR spectrum of H166L exhibits bands with significantly reduced intensity in the same frequency domain compared to those of the bands in the wild-type spectrum (Figure 2, bottom panel), attributing most of the portion of the broad-featured band to the N–H stretching mode of His166 in its imidazolium form (cationic form). It should be

noted that the spectrum of H166L (purple line in Figure 2) still exhibits a positive feature at 2800–2400 cm^{-1} , suggesting the presence of X–H stretching vibrations under strong hydrogen bonds. Interestingly, the purple spectrum resembles that of the wild type, though H166L lacks His at position 166. While this result may sound contradictory, one possible interpretation is that another His residue accepts protons in H166L, but not in the wild type. Upon formation of M, the proton released from the Schiff base is transferred, but in the case of H166L, the proton acceptor must be different from its natural acceptor (His166). The new proton transfer in H166L may directly or indirectly result in partial protonation of one of the remaining His residues, even though that residue is not protonated in the wild type.

Effect of Replacement of His166 on the FTIR Changes and Direction of PSB Deprotonation in SRI.

If His166 accepts a proton from the PSB and participates in the hydrogen bonding network alterations upon formation of M, the H166L mutation is expected to cause perturbations of the vibrational modes of other residues in the M-minus-SRI FTIR spectrum. As described above, mutations of the other three histidines (H34A, H135A, and H221A) caused almost no perturbations in the N–H stretching vibrational modes in the 2800–2400 cm^{-1} domain (Figure 2). Consistent with this notion, these mutants exerted almost no influence in the 1800–800 cm^{-1} domain of the spectrum (data shown for H135A in Figure 4, top red trace), indicating that these histidine residues are not involved in hydrogen bonding alterations upon the conversion from SRI to the M state. His135 is the only one of the three histidines that is predicted to be located near the chromophore (specifically near the β -ionone ring) on the basis of the crystal structure of SRI^{25,26} and therefore is likely to contribute to spectral tuning of the absorption maximum (λ_{max}) of SRI. In fact, H135A exhibits a ~ 25 nm blue shift relative to wild-type SRI (data not shown), which is reflected in the M-minus-SRI difference FTIR spectra of H135A as the ~ 8 cm^{-1} upshift of the C=C stretching modes (1519 from 1511 cm^{-1}) compared to that of the wild type (Figure 4), in agreement with the empirical inverse correlation of the λ_{max} and the frequency of the C=C stretching vibrational

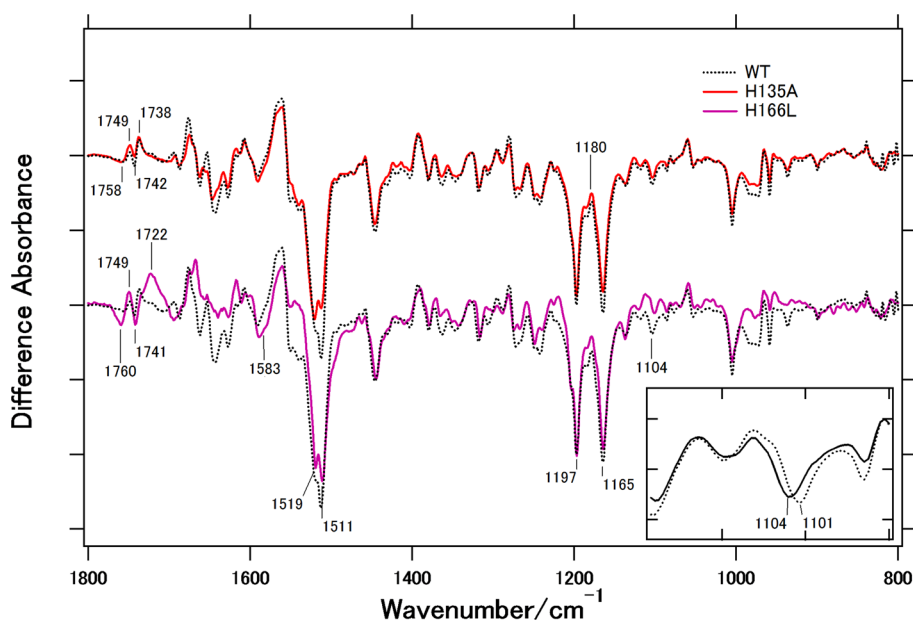


Figure 4. M-minus-SRI difference FTIR spectra of the SRI–HtrI complex measured at pH 5.5 for H135A (red) and H166L (purple) mutant proteins and the wild type (···) of the SRI in complex with HtrI₁₄₇.

mode. Otherwise, almost no appreciable changes are seen in the spectral shape of H135A compared to that of the wild type except for differences in the amplitude of the bands in the amide I and II regions (1700–1600 and 1600–1500 cm^{-1} , respectively), where strong absorbance by these bands in the absolute spectrum can compromise the linearity in the difference spectrum. The striking resemblance of the spectral shape of H135A, H34A, and H221A compared to that of wild-type SRI suggests that these residues are involved in neither the intramolecular proton transfer nor any alterations in the hydrogen bonding network in the SRI-to-M conversion.

In contrast, H166L exhibits spectral perturbations in the difference FTIR spectrum compared to that of wild-type SRI in the 1800–800 cm^{-1} domain (Figure 4, bottom purple trace). The 1104 cm^{-1} band on the negative side of the spectrum in the wild type, which shows a shift to 1101 cm^{-1} upon ^{15}N labeling of histidine (Figure 4, inset), is largely weakened in H166L, suggesting the vibrational mode arises from His166. The assignment is in agreement with the previous observation of the vibrational modes of a model compound of imidazole (MeIm) in the neutral form showing two C–N stretch modes at 1104 and 1087 cm^{-1} , corresponding to the modes containing the unprotonated and protonated nitrogen of the neutral form of imidazole, respectively, the former of which was unaffected upon deuteration.²³ Likewise, the 1104 cm^{-1} band on the negative side of the spectrum of the wild type is unaffected by deuteration (data not shown). It should be noted that the positional assignment of vibrational bands needs special care if protein structures are modified by mutation. This is the case for H166L, for which light-induced spectra differ significantly from that of the wild type. We conclude the residue is His166 from the spectral identity of His mutants other than His166, as well as the case in Figure 2. Thus, the presence of the C–N stretching mode on the negative side of the spectrum is one strong piece of evidence that His166 in the initial state is in the neutral form, which is capable of being protonated as the SB is deprotonated upon formation of M.

Other changes in H166L compared to the wild type in the M-minus-SRI spectrum are likely to be caused by alterations in the hydrogen bonding interactions and conformational changes as a result of the H166 mutation. The significant deviations in the spectral shapes in the amide I region (1700–1600 cm^{-1}) between the wild type and H166L, which reflect the protein backbone conformational changes, indicate differences in conformational changes between the two proteins. Such differences as the proteins convert from the initial state to the M state are expected from the inverted conformer explanation of the inverted signaling and outward direction of Schiff base proton transfer from H166L.^{7,8,15}

Another notable difference between the wild type and H166L is the newly appearing prominent band at 1722 cm^{-1} on the positive side that can be assigned to the C=O stretching vibrational mode of a carboxylate residue protonated upon formation of M. This assignment may be validated also by bands on the negative side that can be attributed to asymmetric O–C–O stretch mode of carboxylate groups near 1583 cm^{-1} , though the symmetric O–C–O stretch mode is unclear at 1450–1350 cm^{-1} . The change in protonation of a carboxylic group upon formation of M indicates that it substitutes for His166 as a proton acceptor from the PSB. The PSB deprotonation in formation of the M state of H166L is likely to have occurred in view of the diminished intensity of the chromophore's vibrational modes on the positive side (near 1180 cm^{-1} for the 13-*cis* configuration),

the feature characteristic of the deprotonated SB that is seen also in the wild type and in other histidine mutants because the decreased degree of π electron delocalization reduces the polarity of the chromophore.

Although attribution of the 1722 cm^{-1} bands is yet to be performed, the only two carboxylate residues near the PSB are Asp76 and Asp201 (corresponding to Asp85 and Asp212 of BR, respectively), candidates for accepting the proton because the PSB is released outward in the H166L mutant and Asp76 and Asp201 are expected to be outwardly located.

The direction of the SB deprotonation that occurs in the microsecond to millisecond time domain has been monitored by photocurrent measurements.^{7,10} The acidic form of SRI deprotonates to the CP side of the protein where His166 is located, as evidenced by the rise of a negative photocurrent in $\sim 200 \mu\text{s}$ (Figure 5, black line).⁷ As previously shown,⁷ in the

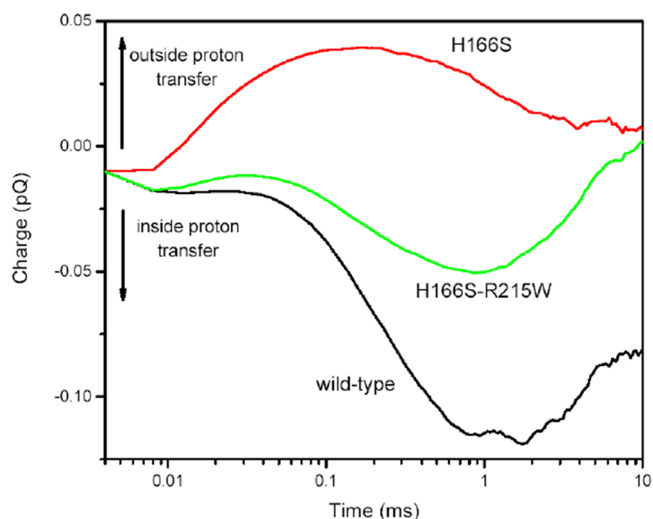


Figure 5. Flash-induced charge movements in the wild-type SRI–HtrI complex (black), the phototaxis signal-inverted H166S mutant (red), and the phenotypically wild-type H166S/R215W double mutant (green) at pH 7.0. Similar measurements were used to calculate the charge shift ratio of the same mutants by Sineshchekov et al.⁷ to establish the charge movement inversion and suppression effect confirmed here.

SRI/H166S–HtrI complex, the negative photocurrent is inverted into a positive one (i.e., movement of a proton toward the EC side) rising in $\sim 20 \mu\text{s}$ (Figure 5, red line), indicating the presence of an alternative proton acceptor of the SB on the EC side. Conversely, His166 was found to contribute to directing the SB deprotonation toward the CP side. However, even in the absence of His166 (in the H166S background), redirection of SB deprotonation to the CP side can be restored by an additional mutation, R215W, in SRI (ref 7 and Figure 5, green line), a suppressor mutant known to revert the repellent phototaxis signaling phenotype of SRI–HtrI mutant complexes into an attractant response.²⁷ Thus, these results confirm the two-conformer model^{7,8} in which the factor that directs the SP deprotonation to the CP side is not the presence of His166, but rather the conformation of SRI responsible for attractant signaling as is the case in the wild type and H166S/R215W, whereas the conformation responsible for repellent signaling directs the SB deprotonation to the EC side.^{7,8}

DISCUSSION

We conclude that the broad band with subpeaks in the 2800–2400 cm^{-1} domain appearing concurrently with SB deprotonation in the acidic form of SRI, the form physiologically active in attractant phototaxis, was found to originate from the N–H stretch modes of the imidazole group of His166. The appearance of a number of subpeaks on the background of the broad feature is therefore not due to the presence of multiple histidine residues undergoing protonation changes but rather can be ascribed to band separation due to the Fermi resonance of overtones and combinations of imidazole ring modes with the N–H stretching vibration that have been pointed out in previous studies of imidazole groups in the histidine of Q_A upon photoreduction by PSII.^{23,24} Because these band patterns appear in the model compound, MeIm, only at pH values well below the pK_a for the transition from the neutral form (MeIm-H) to the cationic form (MeIm- H_2^+) (Figure 3), the most plausible explanation for the appearance of the positive bands near 2800–2500 cm^{-1} is that the imidazole group of His166 becomes the imidazolium (cationic) form upon SB deprotonation. Thus, His166 can be assigned as the proton acceptor of the SB upon formation of M in the wild-type attractant signaling SRI–HtrI complex.

This conclusion is in agreement with the prediction that His166 is located in the vicinity of the SB on the CP side on the basis of the corresponding residue position in the crystal structure of SRII^{25,26} and also with the previous observations that the amplitudes of the M-state absorption (~ 400 nm) are greatly reduced by all seven of the tested mutations of His166,¹⁵ and that SB deprotonation of wild-type SRI in complex with HtrI is toward the CP side of the protein.⁷ Furthermore, as reported previously⁷ and shown in Figure 5, the substitution of Ser for His166 inverts the SB deprotonation to the EC side. Therefore, an alternative proton acceptor exists. The appearance of a vibrational band at 1722 cm^{-1} in the M-minus-SRI spectrum of H166L that can be attributed to a C=O stretching vibrational mode of a protonated carboxyl group suggests the proton acceptor is a carboxyl residue (Figure 4b). Asp76, which corresponds to the Schiff base proton acceptor Asp85 in BR, is a strong candidate, but the λ_{max} of the SRI–HtrI₁₄₇ complex is almost unaffected by H166L and H166S mutations,¹⁵ a result more consistent with Asp76 remaining protonated in the unphotolyzed state in these mutants. Asp201, a carboxylate in the vicinity of the PSB expected to be on the EC side, is a second candidate as a proton acceptor of the PSB when His166 is eliminated by mutation. It is noted that the residual positive feature at 2800–2400 cm^{-1} may suggest partial protonation of one of the remaining His residues in the H166L mutant.

Despite the fact that the PSB proton acceptors are present on both the CP and EC side, the factor that determines the directionality of the PSB deprotonation is not the availability of the acceptor residues, because even in the absence of His166 CP-directed deprotonation of the PSB is observed when the R215A mutation is introduced into the H166S background, ruling out the possibility that His166 is an unequivocal determinant for the CP-directed PSB deprotonation. Thus, the opposite proton release direction is a consequence rather than a cause of the altered conformational state of SRI induced by the H166S mutation. That is, the direction of the PSB deprotonation is governed by which of the two alternative conformers is present in the unphotolyzed state, namely, the attractant or the repellent signaling receptor conformers, which show CP- or EC-directed PSB deprotonations, respectively.^{7,8} Note that the direction of

charge movement provides a convenient assay for the attractant and repellent signaling conformers of the wild-type SRI–HtrI complex, but mutants in which Schiff base proton transfer is greatly altered or does not occur and yet phototaxis is intact rule out the possibility that the proton transfer event itself is a cause of the response. The H166L/S mutation in SRI has been shown to transform the attractant signaling wild-type SRI into a repellent signaling photoreceptor (inverter mutation), whereas the R215A mutation reverts the inverted phenotype into an attractant receptor (suppressor mutation).^{15,27,28} Moreover, the attractant and the repellent forms of SRI have been shown to undergo opposite changes in conformation as monitored by helix F displacement.⁹

Nevertheless, in view of the attenuation of the CP-directed photocurrent upon PSB deprotonation in SRI H166S/R215A compared to that in wild-type SRI (Figure 5), His166 may facilitate the CP-directed deprotonation. This role may be relevant for biasing the conformation toward the kinase-activating unphotolyzed state making SRI an attractant signaling photoreceptor for orange-red light. In any case, the functional importance of His166 is evident in that it is conserved among SRI homologues not only in the related halophilic archaeon *Halobacterium valismortis* and *Haloarcula marismortui* but also in SRI in the eubacterium *Salinibacter ruber*.^{29,30}

The involvement of histidine residues in an intramolecular proton relay in microbial rhodopsins has begun to appear as the number of new rhodopsin members has grown explosively. For example, proteorhodopsin, found in abundance in marine bacteria,³¹ has conserved residue His75 situated in the vicinity of the PSB counterion and the proton acceptor Asp97 and was found to release a proton concurrently with the protonation of Asp97 by the PSB.³²

However, direct observations of transient protonation changes of histidine residues have been difficult to make. Using FTIR spectroscopy, complexity is often encountered in the assignment of minute vibrational modes among the crowd of numerous other bands in the frequency domain between 1800 and 800 cm^{-1} . This problem was overcome in this investigation by focusing on the Fermi resonance modes of the N–H stretch modes of the histidine side chain, which appear in a lower-frequency region (2800–2400 cm^{-1}) than the dominant O–H stretching vibrational modes of water molecules in the case of His166 and 4-methylimidazole due to strong hydrogen bonding interaction upon protonation. As Fermi resonance vibrational modes of amino acid residue side chains in the 2800–2400 cm^{-1} domain have been reported not only for the N–H stretch of His^{23,24} but also for the O–H stretch of Tyr,³³ analysis of bands in this frequency domain will allow identification by difference FTIR spectroscopy of yet uninvestigated roles of amino acid residues in protein functions.

AUTHOR INFORMATION

Corresponding Author

*Department of Frontier Materials, Nagoya Institute of Technology, Showa-ku, Nagoya 466-8555, Japan. Phone and fax: 81-52-735-5207. E-mail: kandori@nitech.ac.jp.

Present Address

[†]Y.F.: Department of Life and Coordination-Complex Molecular Science, Institute for Molecular Science, Myodaiji, Okazaki 444-8585, Japan.

Funding

This work was supported by grants from the Japanese Ministry of Education, Culture, Sports, Science and Technology to H.K. (25104009) and by Grant R01GM027750 from the National Institute of General Medical Sciences and Endowed Chair AU-0009 from the Robert A. Welch Foundation to J.L.S.

Notes

The authors declare no competing financial interest.

ABBREVIATIONS

SB, Schiff base; PSB, protonated Schiff base; BR, bacteriorhodopsin; EC, extracellular; CP, cytoplasmic; SR, sensory rhodopsin; ATR, attenuated total reflection; MeIm, 4-methylimidazole.

REFERENCES

- (1) Spudich, J. L. (2006) The multitasking microbial sensory rhodopsins. *Trends Microbiol.* 14, 480–487.
- (2) Jung, K. H. (2007) The distinct signaling mechanisms of microbial sensory rhodopsins in Archaea, Eubacteria and Eukarya. *Photochem. Photobiol.* 83, 63–69.
- (3) Klare, J. P., Chizhov, I., and Engelhard, M. (2008) Microbial rhodopsins: Scaffolds for ion pumps, channels, and sensors. *Results Probl. Cell Differ.* 45, 73–122.
- (4) Ernst, O. P., Lodowski, D. T., Elstner, M., Hegemann, P., Brown, L. S., and Kandori, H. (2014) Microbial and animal rhodopsins: Structure, functions, and molecular mechanisms. *Chem. Rev.* 114, 126–163.
- (5) Haupts, U., Tittor, J., and Oesterhelt, D. (1999) Closing in on bacteriorhodopsin: Progress in understanding the molecule. *Annu. Rev. Biophys. Biomol. Struct.* 28, 367–399.
- (6) Lanyi, J. K. (2004) Bacteriorhodopsin. *Annu. Rev. Physiol.* 66, 665–688.
- (7) Sineshchekov, O. A., Sasaki, J., Phillips, B. J., and Spudich, J. L. (2008) A Schiff base connectivity switch in sensory rhodopsin signaling. *Proc. Natl. Acad. Sci. U.S.A.* 105, 16159–16164.
- (8) Sineshchekov, O. A., Sasaki, J., Wang, J., and Spudich, J. L. (2010) Attractant and repellent signaling conformers of sensory rhodopsin-transducer complexes. *Biochemistry* 49, 6696–6704.
- (9) Sasaki, J., Tsai, A. L., and Spudich, J. L. (2011) Opposite displacement of helix F in attractant and repellent signaling by sensory rhodopsin-Htr complexes. *J. Biol. Chem.* 286, 18868–18877.
- (10) Sineshchekov, O. A., and Spudich, J. L. (2004) Light-induced intramolecular charge movements in microbial rhodopsins in intact *E. coli* cells. *Photochem. Photobiol. Sci.* 3, 548–554.
- (11) Bergo, V., Spudich, E. N., Scott, K. L., Spudich, J. L., and Rothschild, K. J. (2000) FTIR analysis of the SII540 intermediate of sensory rhodopsin II: Asp73 is the Schiff base proton acceptor. *Biochemistry* 39, 2823–2830.
- (12) Furutani, Y., Takahashi, H., Sasaki, J., Sudo, Y., Spudich, J. L., and Kandori, H. (2008) Structural changes of sensory rhodopsin I and its transducer protein are dependent on the protonated state of Asp76. *Biochemistry* 47, 2875–2883.
- (13) Kitade, Y., Furutani, Y., Kamo, N., and Kandori, H. (2009) Proton release group of pharaonis phoborhodopsin revealed by ATR-FTIR spectroscopy. *Biochemistry* 48, 1595–1603.
- (14) Sasaki, J., Takahashi, H., Furutani, Y., Kandori, H., and Spudich, J. L. (2011) Sensory rhodopsin-I as a bidirectional switch: Opposite conformational changes from the same photoisomerization. *Biophys. J.* 100, 2178–2183.
- (15) Zhang, X. N., and Spudich, J. L. (1997) His166 is critical for active-site proton transfer and phototaxis signaling by sensory rhodopsin I. *Biophys. J.* 73, 1516–1523.
- (16) Chen, X., and Spudich, J. L. (2002) Demonstration of 2:2 stoichiometry in the functional SRI-HtrI signaling complex in *Halobacterium* membranes by gene fusion analysis. *Biochemistry* 41, 3891–3896.

- (17) Shimono, K., Furutani, Y., Kamo, N., and Kandori, H. (2003) Vibrational modes of the protonated Schiff base in pharaonis phoborhodopsin. *Biochemistry* 42, 7801–7806.
- (18) Furutani, Y., Kamada, K., Sudo, Y., Shimono, K., Kamo, N., and Kandori, H. (2005) Structural changes of the complex between pharaonis phoborhodopsin and its cognate transducer upon formation of the M photointermediate. *Biochemistry* 44, 2909–2915.
- (19) Kamada, K., Furutani, Y., Sudo, Y., Kamo, N., and Kandori, H. (2006) Temperature-dependent interactions between photoactivated pharaonis phoborhodopsin and its transducer. *Biochemistry* 45, 4859–4866.
- (20) Spudich, J. L. (1994) Protein-protein interaction converts a proton pump into a sensory receptor. *Cell* 79, 747–750.
- (21) Rath, P., Spudich, E., Neal, D. D., Spudich, J. L., and Rothschild, K. J. (1996) Asp76 is the Schiff base counterion and proton acceptor in the proton-translocating form of sensory rhodopsin I. *Biochemistry* 35, 6690–6696.
- (22) Rath, P., Olson, K. D., Spudich, J. L., and Rothschild, K. J. (1994) The Schiff base counterion of bacteriorhodopsin is protonated in sensory rhodopsin I: Spectroscopic and functional characterization of the mutated proteins D76N and D76A. *Biochemistry* 33, 5600–5606.
- (23) Noguchi, T., Inoue, Y., and Tang, X. S. (1999) Structure of a histidine ligand in the photosynthetic oxygen-evolving complex as studied by light-induced fourier transform infrared difference spectroscopy. *Biochemistry* 38, 10187–10195.
- (24) Noguchi, T., Inoue, Y., and Tang, X. S. (1999) Hydrogen bonding interaction between the primary quinone acceptor QA and a histidine side chain in photosystem II as revealed by Fourier transform infrared spectroscopy. *Biochemistry* 38, 399–403.
- (25) Luecke, H., Schobert, B., Lanyi, J. K., Spudich, E. N., and Spudich, J. L. (2001) Crystal structure of sensory rhodopsin II at 2.4 Å: Insights into color tuning and transducer interaction. *Science* 293, 1499–1503.
- (26) Royant, A., Nollert, P., Edman, K., Neutze, R., Landau, E. M., Pebay-Peyroula, E., and Navarro, J. (2001) X-ray structure of sensory rhodopsin II at 2.1-Å resolution. *Proc. Natl. Acad. Sci. U.S.A.* 98, 10131–10136.
- (27) Jung, K. H., and Spudich, J. L. (1998) Suppressor mutation analysis of the sensory rhodopsin I-transducer complex: Insights into the color-sensing mechanism. *J. Bacteriol.* 180, 2033–2042.
- (28) Sasaki, J., Phillips, B. J., Chen, X., Van Eps, N., Tsai, A. L., Hubbell, W. L., and Spudich, J. L. (2007) Different dark conformations function in color-sensitive photosignaling by the sensory rhodopsin I-HtrI complex. *Biophys. J.* 92, 4045–4053.
- (29) Kitajima-Ihara, T., Furutani, Y., Suzuki, D., Ihara, K., Kandori, H., Homma, M., and Sudo, Y. (2008) *Salinibacter* sensory rhodopsin: Sensory rhodopsin I-like protein from a eubacterium. *J. Biol. Chem.* 283, 23533–23541.
- (30) Sudo, Y., Yuasa, Y., Shibata, J., Suzuki, D., and Homma, M. (2011) Spectral tuning in sensory rhodopsin I from *Salinibacter ruber*. *J. Biol. Chem.* 286, 11328–11336.
- (31) de la Torre, J. R., Christianson, L. M., Beja, O., Suzuki, M. T., Karl, D. M., Heidelberg, J., and DeLong, E. F. (2003) Proteorhodopsin genes are distributed among divergent marine bacterial taxa. *Proc. Natl. Acad. Sci. U.S.A.* 100, 12830–12835.
- (32) Bergo, V. B., Sineshchekov, O. A., Kralj, J. M., Partha, R., Spudich, E. N., Rothschild, K. J., and Spudich, J. L. (2009) His-75 in proteorhodopsin, a novel component in light-driven proton translocation by primary pumps. *J. Biol. Chem.* 284, 2836–2843.
- (33) Iwata, T., Watanabe, A., Iseki, M., Watanabe, M., and Kandori, H. (2011) Strong donation of the hydrogen bond of tyrosine during photoactivation of the BLUF domain. *J. Phys. Chem. Lett.* 2, 1015–1019.